Optothermal Properties of Fibers. III. Optical Anisotropy in Nylon 66 Fibers as a Function of Annealing Process

I. M. FOUDA,[1,*] M. M. EL-NICKLAWY,[2] E. M. NASR,[2] and R. M. EL-AGAMY[2]

[1]Physics Department, Faculty of Science, Mansoura University, Mansoura, Egypt, and [2]Physics Department, Faculty of Science, Helwan University, Cairo, Egypt

SYNOPSIS

Nylon 66 (ICI Polyamide 66, Carded & Combed Top) fibers were annealed in the temperature range 80–180°C for 1–10 h. Refractive indices and birefringence were measured interferometrically. Two independent techniques were used to study the optical anisotropy in these fibers. The first technique was to study the effect of annealing on the swelling properties of fibers from its diffraction pattern using a He—Ne laser beam. The second was the application of multiple-beam Fizeau fringes in transmission to determine the skin and core refractive indices and double refraction of annealing samples. The application was carried out using multiple-beam Fizeau fringes in transmission to determine Cauchy's constants and the dispersive coefficient for the fiber layers. The resulting data were used to calculate the mean polarizability per unit volume and the isotropic refractive indices. Behavior of optical properties at different annealing conditions is discussed. The results obtained clarify the new reorientation, and each layer change occurred due to annealing at different conditions. Microinterferograms and curves are given for illustration. © 1996 John Wiley & Sons, Inc.

INTRODUCTION

Assessment of the optical anisotropy of fibers is of considerable importance, since it provides information about the degree of orientation of a particular molecular system, making its possible to evaluate the effect of any mechanical, thermal, or chemical treatment; knowledge of this kind is of great relevance in the development of modern methods of quality control in many industrial processes.[1]

Swelling of the fiber is another very important tool for the investigation of the structure of the fiber material. When a fiber is immersed in water, the water molecules infiltrate into the fiber and find their way in between the long-chain molecules, hence, pushing them apart. As the fiber-chain molecules are oriented in line with the axis of the fiber and as they are pushed apart, there will be a considerable increase in the diameter of the fiber.[2] Water molecules or liquid molecules can enter the amorphous regions, but not the crystalline region.[3] The value of the swelling factor is an indication of the fiber material, and a higher swelling factor, the greater the amorphous regions.[2]

Part of the modern trend in fiber research is to alter fiber properties. One of the methods for property modification involves the effect of the annealing process at different conditions. Several studies have been reported on the effect of annealing on the structure of synthetic and natural fibers.[4–9] Annealing may be performed with the ends of the sample free or fixed. In the former, the sample shrinks, whereas in the latter case, it retains its length but exerts measurable refractive forces on its fixed ends. Both effects increase with increased annealing temperature.[10]

In this work, first, samples of nylon 66 fibers having different annealing times and different annealing temperatures were measured interferometrically using multiple-beam Fizeau fringes. Second, a diffraction technique was used to evaluate the swelling factors for different liquids. The relationship between the optical parameters and swelling factors with annealing conditions are given.

* To whom correspondence should be addressed.

Journal of Applied Polymer Science, Vol. 60, 1247–1267 (1996)
 CCC 0021-8995/96/091247-21

EXPERIMENTAL AND DISCUSSION

Sample Preparation

Annealing

The nylon 66 fibers were distributed in small glass bottles which were then heated in an electric oven whose temperature was adjusted to be constant to within ±1°C. The samples were annealed at temperature ranging from 80 to 180°C or at different annealing times ranging from 1 to 10 h. The samples were then left to cool at room temperature of 25 ± 1°C. A remarkable limitation occurred due to annealing the samples for 6 h at 180°C; after this condition, the fibers turn to the brittle state for which we cannot use our optical measurements.

Swelling

Fibers were placed in five solvents, water, sodium carbonate solution 20 g for 1 L of water, acetic acid 90% concentration, paraffin oil, and glycerin, at room temperature for 1 h. The examined fibers for swelling were a group of annealed nylon 66 fibers at 120°C for an annealing time of 1–10 h with untreated fiber.

In this work, two different techniques were used to estimate the geometrical parameters of nylon 66 fibers. An optical microscope and the diffraction of a He—Ne laser beam were used to measure the dimensional parameters and the transverse sectional shape.[11,12]

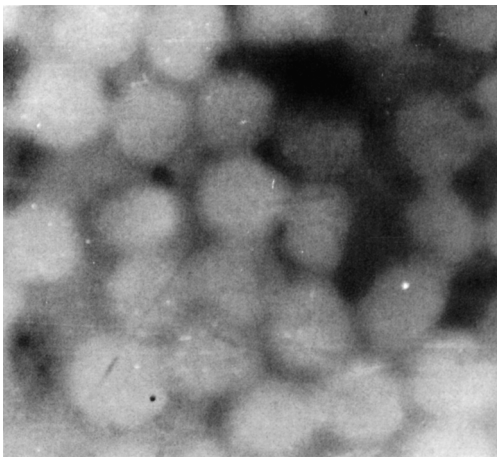

Plate 1 Optical cross section of nylon 66 fibers.

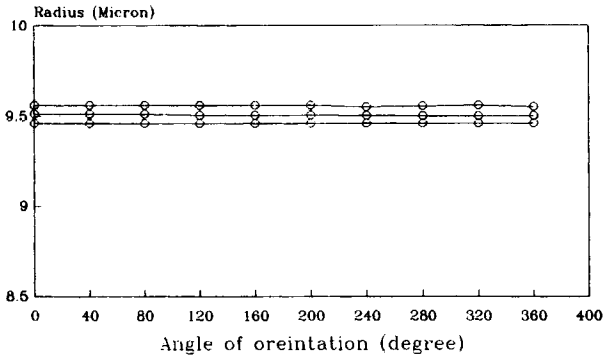

Figure 1 Relation between angle of orientation and fiber radius (microns) for three samples.

Interferometry

The interferometric technique was utilized to study the optical parameters of these fibers. The technique was described in detail previously.[13,14] The change of the refractive indices and birefringence of the fiber layers to the applied different annealing conditions were studied using a wedge interferometer, as discussed elsewhere,[6] to produce multiple-beam Fizeau fringes in transmission. The techniques and relations used in this study are listed below.

Transverse-sectional Shape and Diameter Measurement

Optical Cross-section Method

Plate 1 shows the optically obtained cross-sectional shape of the nylon 66 fibers. The mean diameter was 19 ± 0.2 μm.

Diffraction of He—Ne Laser Beam

In this method, the following formula[11,12] is used:

$$d = \pm\lambda L/x \qquad (1)$$

where d is the fiber thickness, λ = 632.8 nm (the wavelength of the He—Ne laser used); x is the distance from the center of the pattern to the first minimum, and L is the distance between the fiber and the screen on which the diffraction pattern is produced. Figure 1 shows the graphical plot of the cross-sectional shape for three samples. The obtained straight lines mean that the cross section on nylon 66 is circular. The mean fiber diameter was 19 ± 0.2 μm.

Swelling of the Fiber Coefficient

For the determination of the swelling factor of the fibers, Jindricii et al.[15] used a diffraction technique with a laser beam to estimate the diameter before and after swelling in different solvents. The swelling factor was given by applying eq. (1) and the following eq. (2):

$$q = 100(d_s - d_d)/d_d \tag{2}$$

where q is the swelling factor, d_s = swollen diameter, and d_d = dry diameter. Table I gives the experimental values of the swelling factor for untreated and annealed samples of nylon 66 in different solvents.

INTERFEROMETRIC MEASUREMENTS OF THE OPTICAL PARAMETERS

Multiple-beam Fizeau fringes in transmission were used for the determination of the basic optical parameters of nylon 66 fibers.

Determination of the Refractive Indices and Birefringence for the Fiber Layers

For the determination of the refractive index of each layer, n_k, of a cylindrical fiber having m layers of circular cross sections, El-Nicklawy and Fouda[14] derived an expression for the size of the fringe shift ΔZ at any point x along the diameter of a multiskin fiber. In a case having only a skin–core fiber, their expression leads to the following formula:

$$(\lambda/4h)\Delta Z = (n_s^{\parallel} - n_L)(r_s^2 - x^2)^{1/2} + (n_c^{\parallel} - n_s^{\parallel})(r_c^2 - x^2)^{1/2} \tag{3}$$

where $n_s^{\parallel}$ and $n_c^{\parallel}$ are the refractive indices of the skin and core, respectively, for plane-polarized light vibrating parallel to the fiber axis; n_L, the refractive index of the immersion liquid; r_s and r_c, the radii of the skin and core, respectively; h, the liquid interfering spacing; and λ, the wavelength of monochromatic light used. An analogous formula for eq. (3) is used for plane-polarized light vibrating perpendicular to the fiber axis for determination of both $n_s^{\perp}$ and $n_c^{\perp}$.

The Mean Refractive Index n_a

The mean refractive index n_a of nylon 66 fibers, having a core of thickness t_c and refractive index n_c, surrounded by a skin layer of thickness t_s and refractive index n_s, was calculated using the formula[13]

$$n_a = n_c \frac{t_c}{t_f} + n_s \frac{t_s}{t_f} \tag{4}$$

with $t_f = t_s + t_c$, where t_f is the whole fiber thickness.

Refractive Index of Untreated Nylon 66 Fibers

The refractive indices $n_s^{\parallel}$, $n_c^{\parallel}$ and $n_s^{\perp}$, $n_c^{\perp}$ for the fiber layers and also $n_a^{\parallel}$, $n_a^{\perp}$, Δn_s, Δn_c, and Δn_a were determined interferometrically for the untreated sample. Plate 2(a,b) shows microinterferograms of multiple-beam Fizeau fringes in transmission crossing untreated nylon 66 fiber using a monochromatic light (546.1 nm) vibrating (a) parallel and (b) perpendicular to the fiber axis at room temperature of 25 ± 1°C. Table IIgives the experimental values of the refractive indices of the skin, core, and mean of nylon 66 fiber and their birefringence at room temperature.

Table I Values of Swelling Factor for Untreated and Annealed Nylon 66 Fibers in Different Solvents

State	Sodium Carbonate Solution 20 g in 1 L Water	Water	Paraffin Oil	Acetic Acid 90% Concentration	Glycerin
Untreated	10	6.3	14.2	15.3	3.7
120°C 1 h	6.3	8.95	13.2	12.6	3.8
120°C 2 h	5.3	8.95	11.1	12.1	4.2
120°C 4 h	6.3	6.3	14.2	13.7	8
120°C 6 h	6.3	6.3	14.74	12.6	1.37
120°C 8 h	6.3	5.3	14.2	15.3	1.37
120°C 10 h	8.95	6.3	14.2	15.3	5.16

Plate 2 Microinterferograms of multiple-beam Fizeau fringes in transmission crossing unannealed nylon 66 fibers using monochromatic light vibrating (a) parallel and (b) perpendicular to the fiber axis at room temperature of 25 ± 1°C.

Refractive Index–Annealing Time Dependence of Nylon 66 Fibers

The refractive indices $n_s^{\parallel}$, $n_c^{\parallel}$, and $n_s^{\perp}$, $n_c^{\perp}$ for the fiber layers and also their mean values are determined interferometrically at different annealing times. Plate 3(a–f) shows microinterferograms of multiple-beam Fizeau fringes in transmission for nylon 66 fibers at a constant temperature of 160°C with annealing times of 1, 2, 4, 6, 8, and 10 h, respectively. A monochromatic light of wavelength 546.1 nm vibrating parallel to the fiber axis was used.

Figure 2(a–f) shows the behavior of the refractive indices $n_s^{\parallel}$, $n_c^{\parallel}$, and $n_a^{\parallel}$ of annealing nylon 66 fibers,

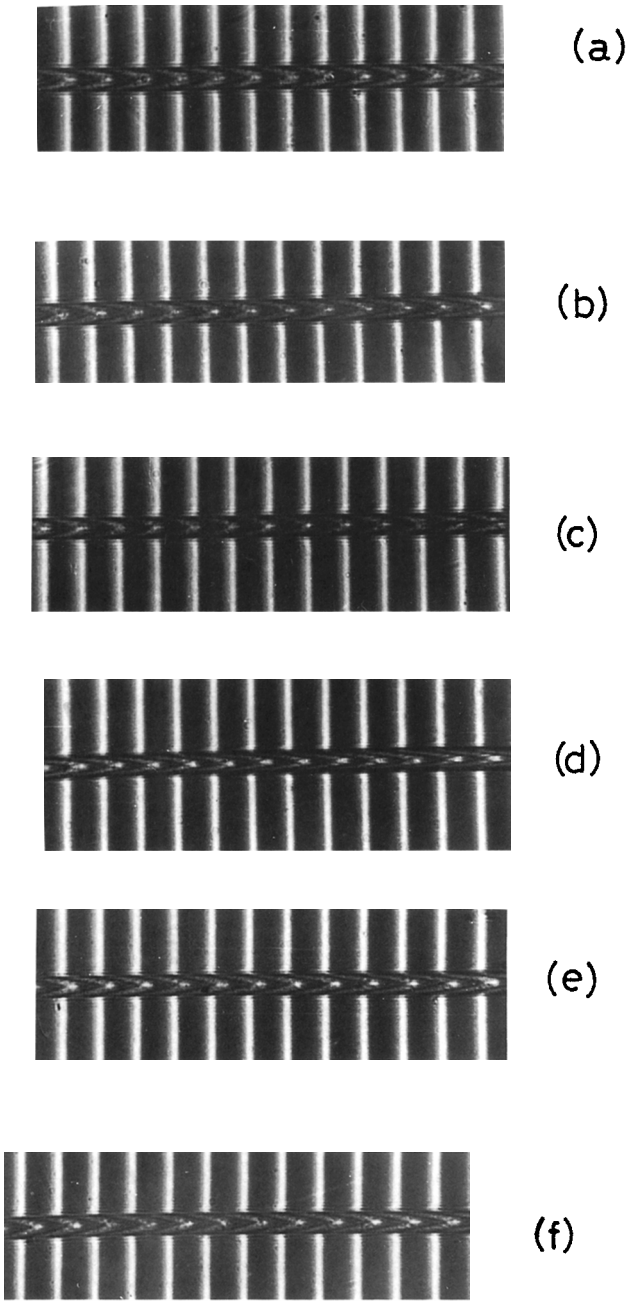

Plate 3 (a–f) Microinterferograms of multiple-beam Fizeau fringes in transmission crossing annealed nylon 66 fibers at a constant temperature of 160°C and different times (1, 2, 4, 6, and 10 h) using monochromatic light vibrating parallel to the fiber axis.

Table II Measured Values of Nylon 66 Fibers at Room Temperature of 25 ± 1°C

Temperature	$n_s^{\parallel}$	$n_s^{\perp}$	Δn_s	$n_c^{\parallel}$	$n_c^{\perp}$	Δn_c	$n_a^{\parallel}$	$n_a^{\perp}$	Δn_a
25°C	1.5794	1.5237	.0557	1.5852	1.528	0.0572	1.5803	1.5244	0.0559

on increasing annealing time at different constant temperatures. It was found that annealing for 1 h for different ranges (80–180°C) leads to increased $n_s^{\parallel}$, $n_c^{\parallel}$, and $n_a^{\parallel}$ in all cases, but there are some transformations that occurred in Figure 2(a,b) which may be attributed to that the mobility of the molecular chains in these directions due to isothermal energy storage have stabilized the increase, as in Figure 2(d–f).

Plate 4(a–f) shows microinterferograms of multiple-beam Fizeau fringes in transmission for nylon 66 fibers at a constant temperature of 160°C with annealing times of 1, 2, 4, 6, 8, and 10 h, respectively. A monochromatic light of wavelength 546.1 nm vibrating perpendicular to the fiber axis was used.

Figure 3(a–f) shows the behavior of $n_s^{\perp}$, $n_c^{\perp}$, and $n_a^{\perp}$ on increasing the time of annealing at constant temperatures for nylon 66 fibers. It was observed that annealing for 1 h from 100–180°C leads to increase of $n_s^{\perp}$, $n_c^{\perp}$, and $n_a^{\perp}$ in all cases, but, in general, annealing periods from 1–4 h consider the change in volume expansion behavior of the amorphous chains (noncrystallizable) and also an increase of the annealing time shows discontinuity in the volume expansion in these directions, which show remarkable orientation to the axial axis (parallel axis).

Refractive Index–Annealing Temperature Dependence of Nylon 66 Fibers

The multiple-beam Fizeau fringes were used to study the thermal change of the refractive index and birefringence of skin and core layers of nylon 66 fibers. The produced fringe shift was measured after the change in annealing temperature within the range 80–180°C with a tolerance of ±1°C, at constant time. Plates 5(a–f) and 6(a–f) are microinterferograms showing the variation of the fringe shift across the nylon 66 fibers at annealing temperatures of 80, 100, 120, 140, 160, and 180°C, respectively, and at a constant time of 1 h. A monochromatic light of wavelength 546.1 nm vibrating parallel plates [5(a–f)] and perpendicular plates [6(a–f)] to the fiber axis was used. Plate 7(a,b) shows microinterferograms of multiple-beam Fizeau fringes in transmission crossing annealed nylon 66 fiber using a monochromatic light vibrating parallel and perpendicular to the fiber axis at an annealing temperature 180°C and time of 6 h. After these conditions, the fiber material turns to the brittle state, which is very difficult to examine with this technique.

Figure 4(a–f) shows the relation of the behavior of $n_s^{\parallel}$, $n_c^{\parallel}$, and $n_a^{\parallel}$ on the increase of the temperature

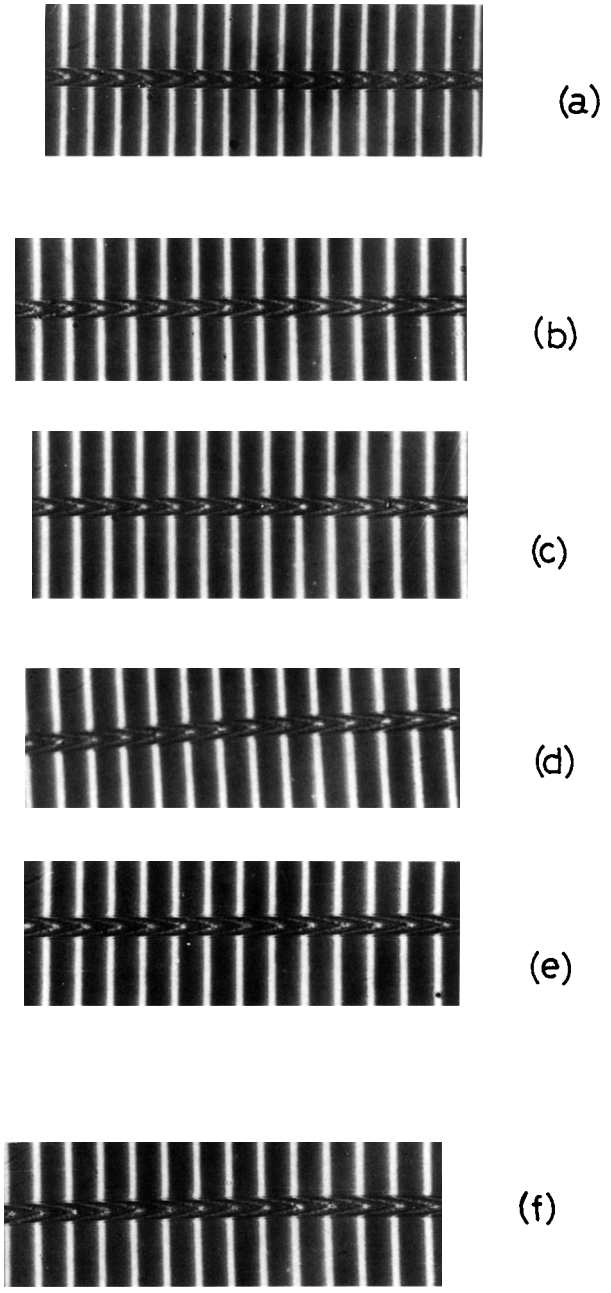

Plate 4 (a–f) Microinterferograms of multiple-beam Fizeau fringes in transmission crossing annealed nylon 66 fibers at a constant temperature of 160°C and different times (1, 2, 4, 6, and 10 h) using monochromatic light vibrating perpendicular to the fiber axis.

of annealing at different constant times. From these curves, we observe a certain characteristic annealing range temperature (100–120°C); after these, the rate increases for $n_s^{\parallel}$, $n_c^{\parallel}$, and $n_a^{\parallel}$. This phenomenon may be due to the change in specific volume behavior and transformation from the glass transition below

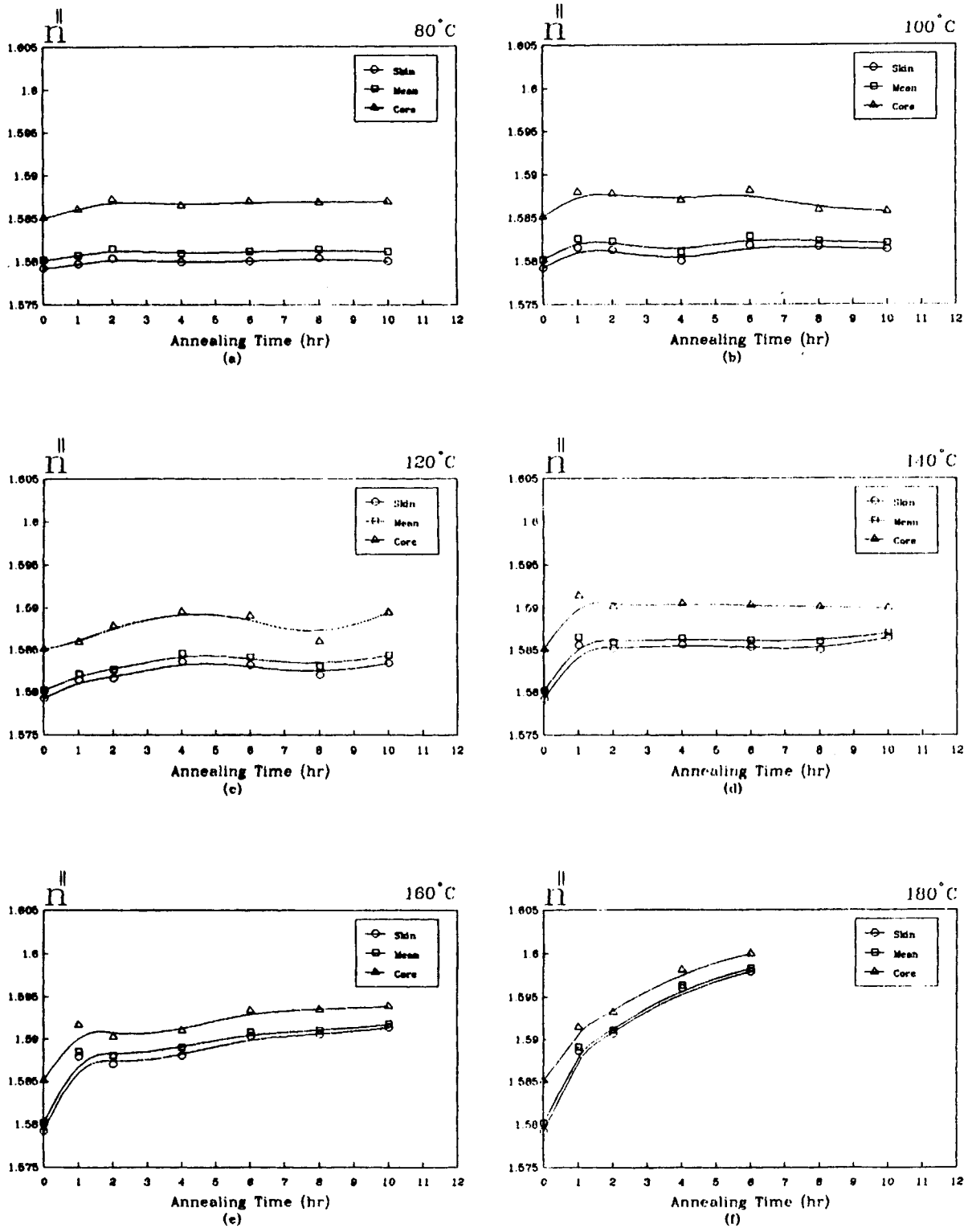

Figure 2 (a–f) Relation between annealing time (1–10 h) and parallel refractive indices at constant annealing temperature (80, 100, 120, 140, 160, and 180°C).

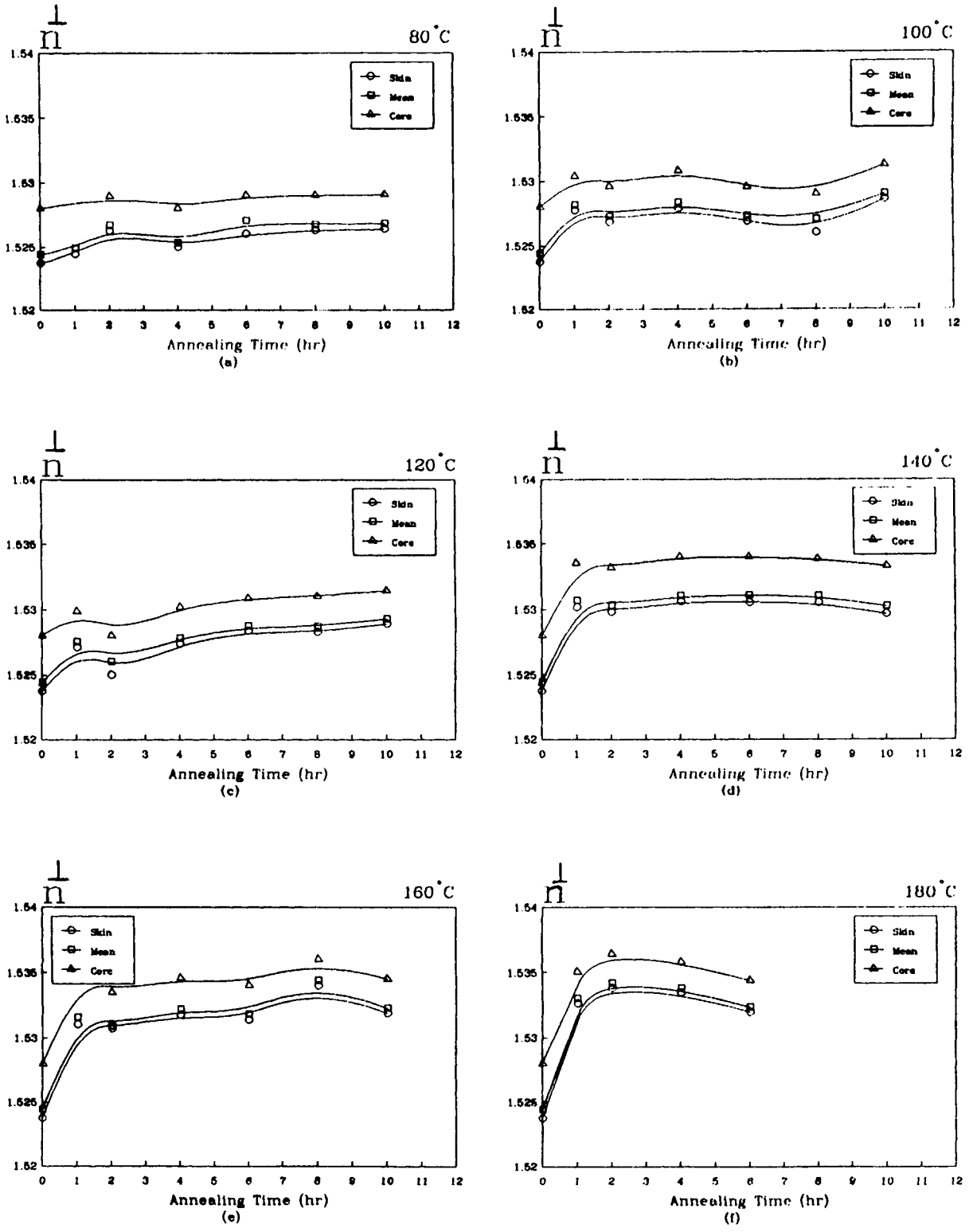

Figure 3 (a–f) Relation between annealing time (1–10 h) and perpendicular refractive indices at constant annealing temperature (80, 100, 120, 140, 160, and 180°C).

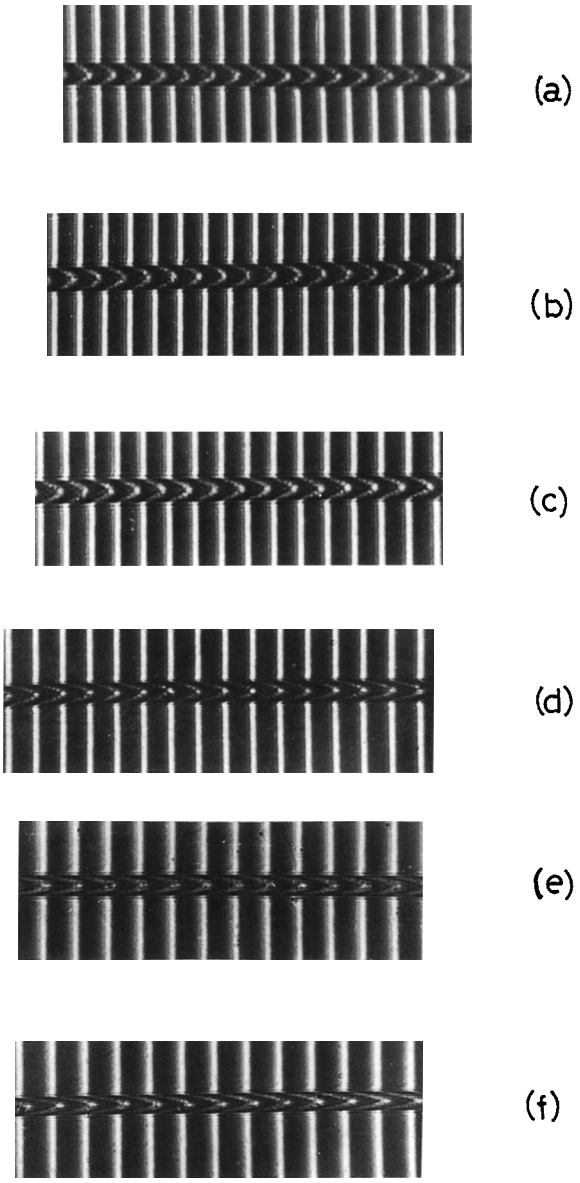

Plate 5 (a–f) Microinterferograms of multiple-beam Fizeau fringes in transmission crossing annealed nylon 66 fibers using monochromatic light vibrating parallel to the fiber axis at annealing temperatures of (a) 80°C, (b) 100°C, (c) 120°C, (d) 140°C, (e) 160°C, and (f) 180°C for a constant annealing time of 1 h.

T_g to soft and rubbery behavior as temperature is increased above T_g.

Figure 5(a–f) shows the relation of the behavior of $n_s^{\perp}$, $n_c^{\perp}$, and $n_a^{\perp}$ on the increase of the temperature of annealing at different constant times. It is clear from the obtained curves that as the temperature of annealing increased we observe a transition state at 100–140°C for these directions ($n_s^{\perp}$, $n_c^{\perp}$, and $n_a^{\perp}$). This transformation change may be due to the change of the crystalline ratio to the amorphous ratio; the obtained new reorientation of the molecules refers to geometrical arrangements of neighboring groups.

Figure 6(a–f) shows the changes of the birefringence Δn_s, Δn_c, and Δn_a due to the increased annealing time at different constant annealing temperatures. From these curves, it was found that with the variation of orientation for skin, core, and mean

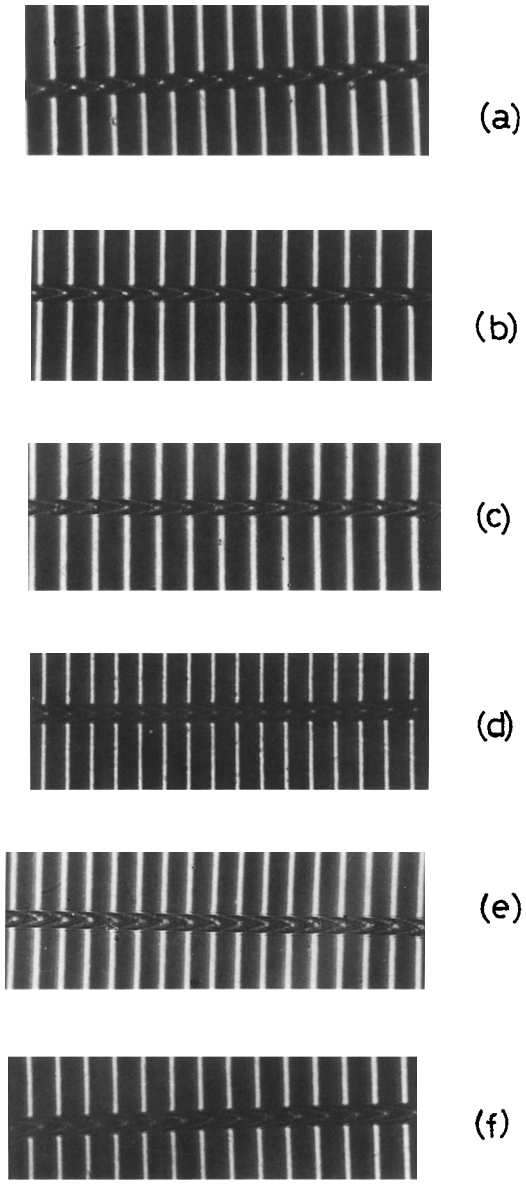

Plate 6 (a–f) Microinterferograms of multiple-beam Fizeau fringes in transmission crossing annealed nylon 66 fibers using monochromatic light vibrating perpendicular to the fiber axis at annealing temperatures of (a) 80°C, (b) 100°C, (c) 120°C, (d) 140°C, (e) 160°C, and (f) 180°C for a constant annealing time of 1 h.

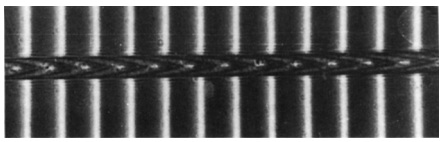

(a)

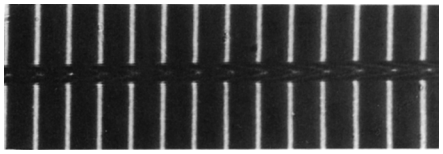

(b)

Plate 7 Microinterferograms of multiple-beam Fizeau fringes in transmission crossing annealed nylon 66 fibers using monochromatic light vibrating (a) parallel and (b) perpendicular to the fiber axis at annealing temperature of 180°C and at time of 6 h.

on annealing from 1 to 4 h a remarkable change for the skin and core orientations is noticed and these may be due to the cohesiveness perserved in both the crystalline and oriented amorphous regions. Also, in Figure 6(e,f), the curves of Δn_s, Δn_c, and Δn_a show a coherency of chain orientations of the skin and core and this may be due to that the crystal blocks move back into the crystallographic register to reform the lamella, especially at high temperature and time of annealing.

Figure 7(a–f) shows changes in the birefringence Δn_s, Δn_c, and Δn_a due to increasing annealing temperatures at different constant annealing times. From these curves, it was found that with the variations of orientation for Δn_s, Δn_c, and Δn_a on annealing at 100–140°C a remarkable change is noticed for the skin, core, and mean; these changes may be due to transformations for the oriented crystallites and oriented amorphous regions to establish a new crystallographic form that depends on the new annealing conditions.

It must be noted also that the changes for the parallel and perpendicular directions for the skin, core, and mean lead to the results obtained in Figures 6 and 7 for all the birefringence mentioned above.

The Dispersion of Nylon 66 Fibers

The dispersion properties of the fibers under test are studied using the well-known Cauchy's formula:

$$n_{(\lambda)} = A + B/\lambda^2 \tag{5}$$

where A and B are Cauchy's constants. The refractive indices $n_{(\lambda)}$ of nylon 66 fibers are measured interferometrically. Figures 8(a–d) and 9(a–d) show the variation of $n_s^{\parallel}$, $n_c^{\parallel}$, $n_a^{\parallel}$, $n_s^{\perp}$, $n_c^{\perp}$, and $n_a^{\perp}$ with $1/\lambda^2$ from which Cauchy's s constants are determined for unannealed and annealed nylon 66 fibers at a constant temperature of 140°C and different annealing times. Table III gives values of Cauchy's constants for both layers of nylon 66 fibers in the two principal directions of vibration of the light.

The Dispersive Coefficient of Nylon 66 Fibers

The dispersive coefficient ($dn/d\lambda$) can be obtained by differentiating eq. (5), i.e.:

$$dn_{(\lambda)}/d\lambda = -2B/\lambda^3 \tag{6}$$

Table IV gives values of the dispersive coefficient for the layer of nylon 66 fibers in the two directions of polarization for the monochromatic light used.

The Polarizability Per Unit Volume

The experimental values of the refractive indices were utilized to obtain the polarizability per unit volume, using the Lorentz–Lorentz equation:

$$P^{\parallel} = 3(n^{\parallel 2} - 1)/4\pi(n^{\parallel 2} + 2) \tag{7}$$

and with an analogous formula for the perpendicular direction. Table V shows the calculated values of polarizability per unit volume and isotropic refractive indices of untreated nylon 66 fiber at room temperature of 25 ± 1°C. Figures 10(a–f) and 11(a–f) give the behavior of the $P_a^{\parallel}$ and $P_a^{\perp}$ for different conditions of annealing.

Isotropic Refractive Index–Annealing Temperature and Time Dependence of Nylon 66 Fibers

The isotropic refractive index of a medium gives information about not only the molecular package but

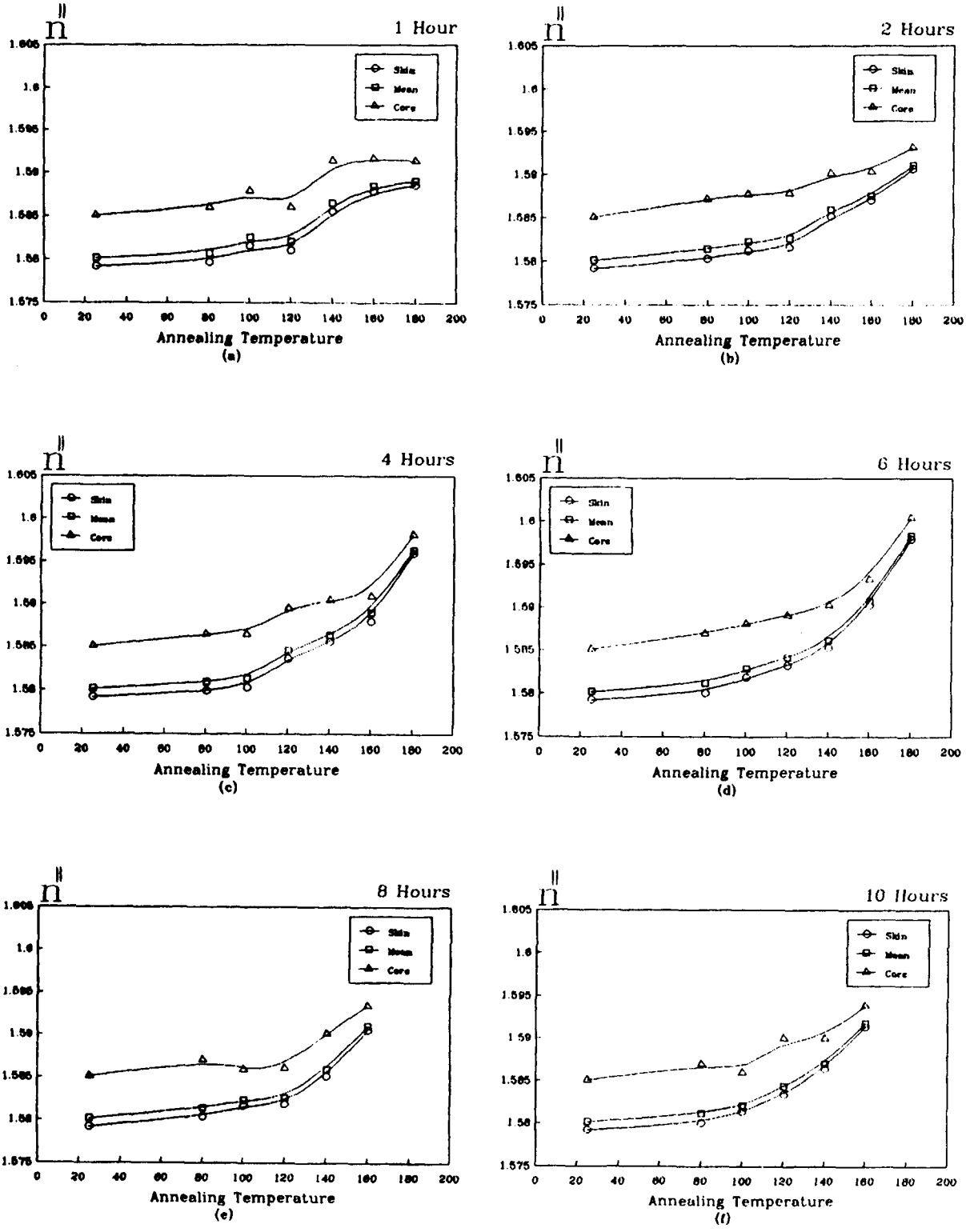

Figure 4 (a–f) Relation between annealing temperature (80–180°C) and parallel refractive indices at constant annealing time (1, 2, 4, 6, 8, and 10 h).

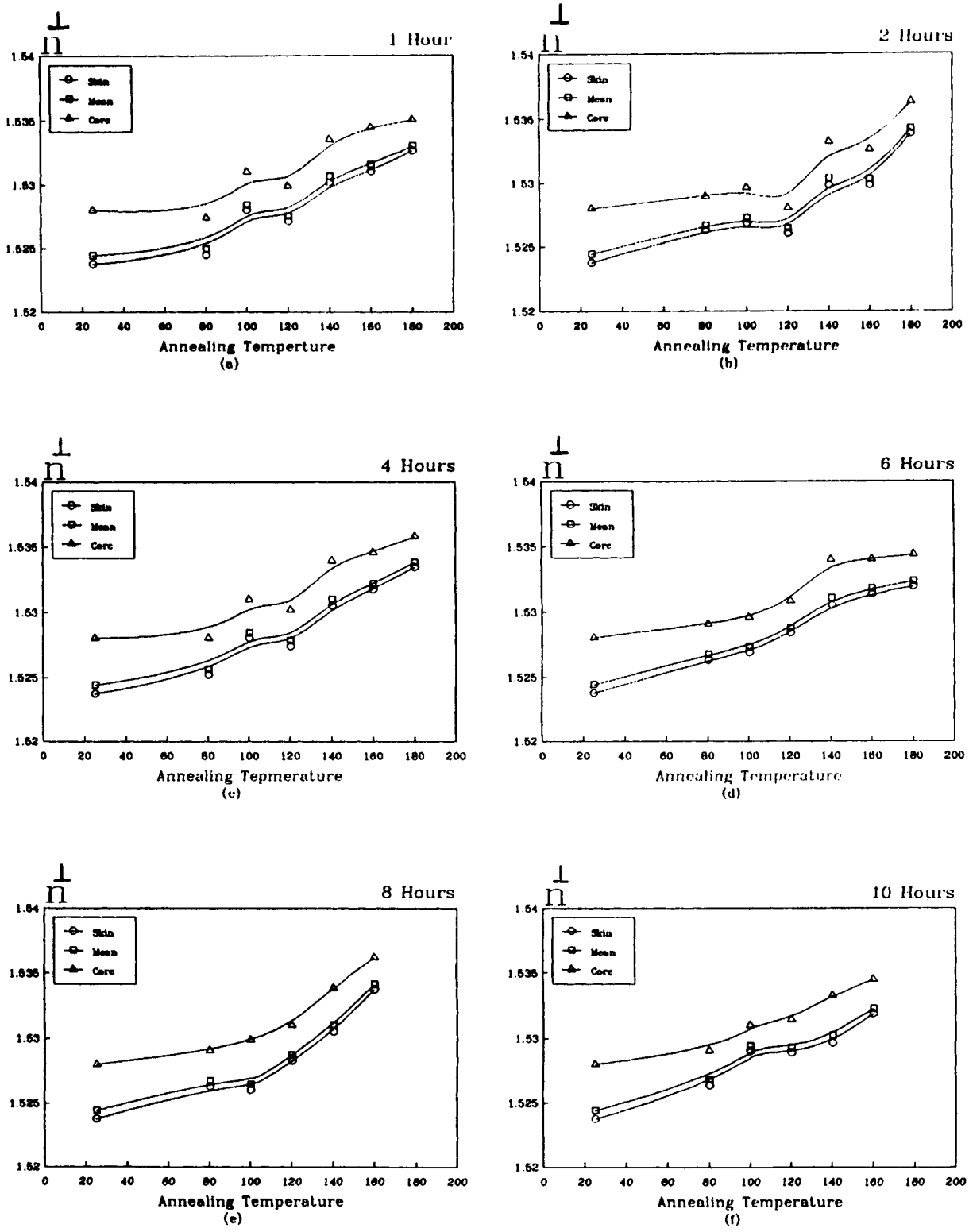

Figure 5 (a–f) Relation between annealing temperature (80–180°C) and perpendicular refractive indices at constant annealing time (1, 2, 4, 6, 8, and 10 h).

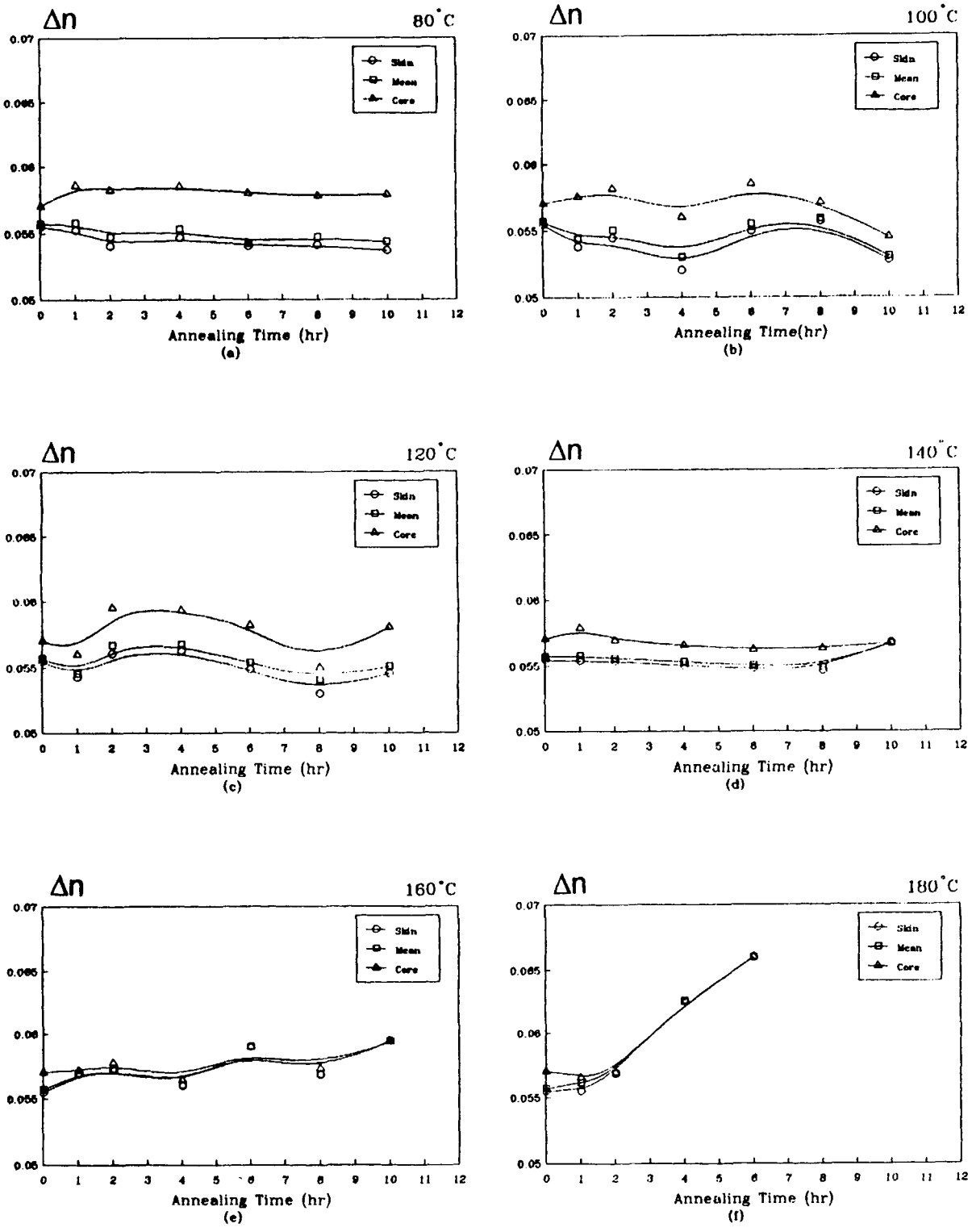

Figure 6 (a–f) Relation between annealing time (1–10 h) and birefringence Δn_s, Δn_c, and Δn_a at constant annealing temperature (80, 100, 120, 140, 160, and 180°C).

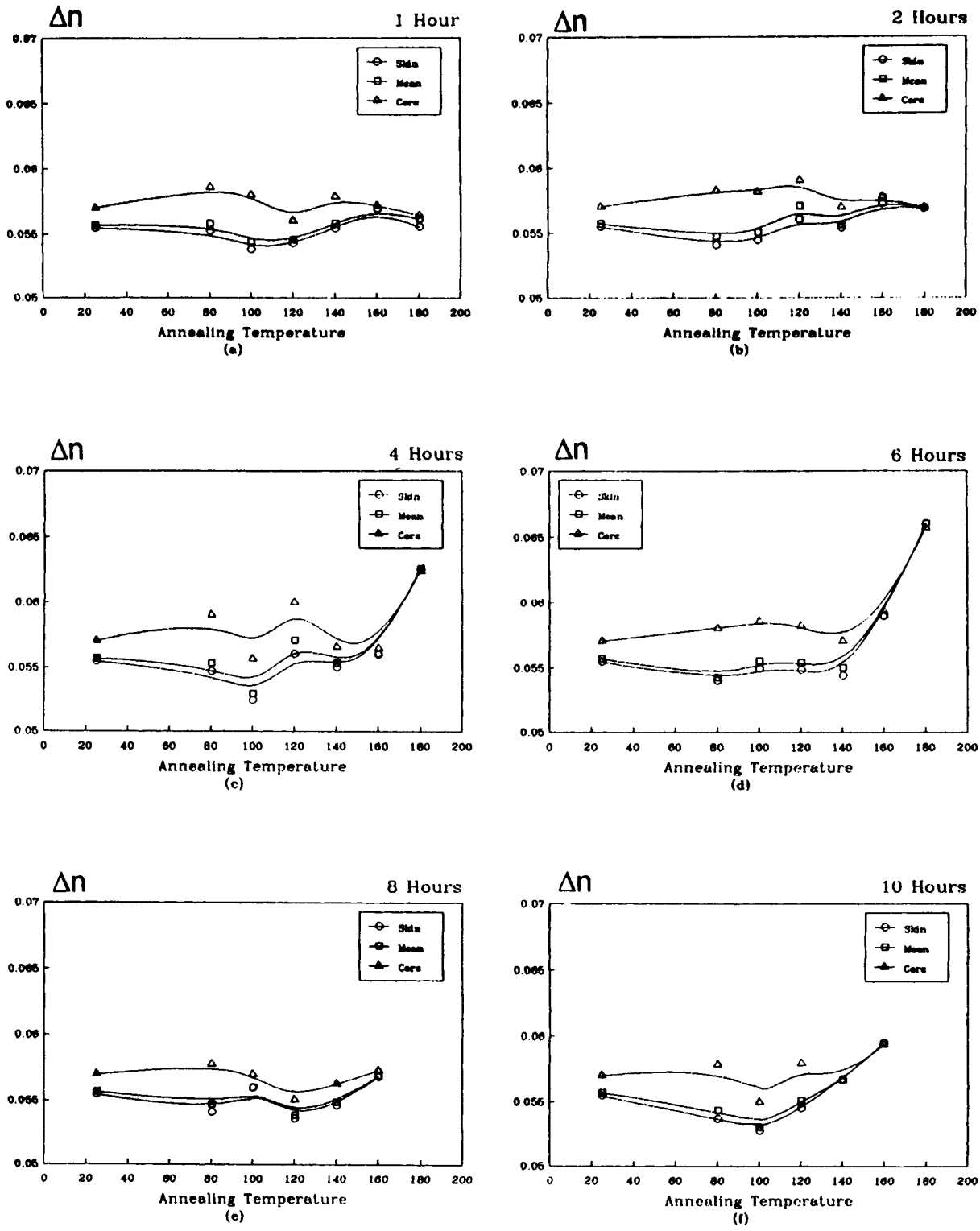

Figure 7 (a–f) Relation between annealing temperature (80–180°C) and birefringence Δn_s, Δn_c, and Δn_a at constant annealing time (1, 2, 4, 6, 8, and 10 h).

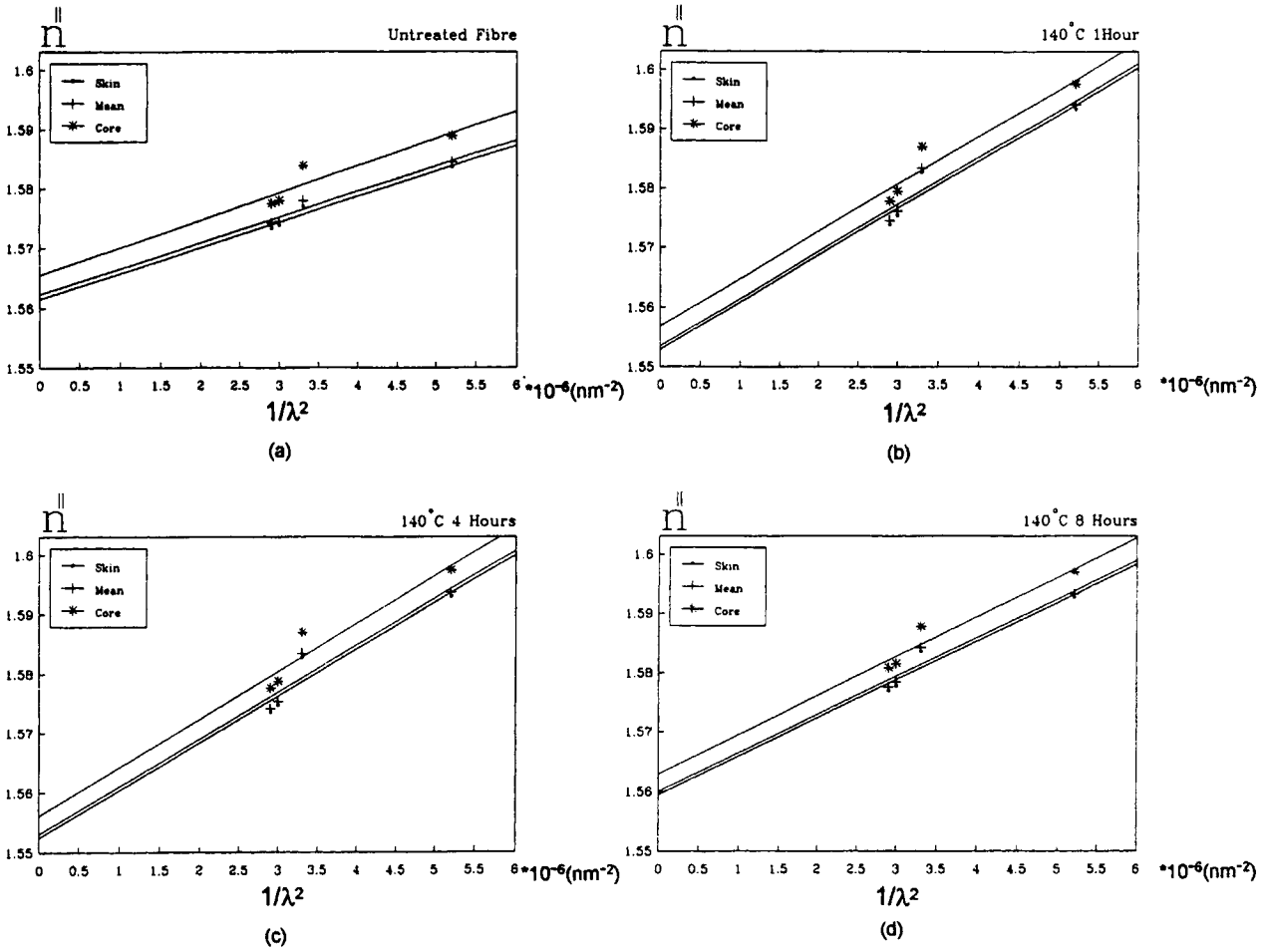

Figure 8 (a–d) Variation of $n_s^{\parallel}$, $n_c^{\parallel}$, and $n_a^{\parallel}$ with $1/\lambda^2$.

Table III Values of Cauchy's Constants for Unannealed and Annealed Nylon 66 Fibers

		Constant "A"		Constant "B" $\times 10^3$ (nm^2)	
State	Layer	$A^{\parallel}$	$A^{\perp}$	$B^{\parallel}$	$B^{\perp}$
Unannealed	Skin	1.5614	1.4988	4.29	7.99
	Mean	1.5623	1.4996	3.64	8.04
	Core	1.5618	1.5016	3.89	8.38
140°C 1 h	Skin	1.5529	1.4995	7.83	8.19
	Mean	1.5538	1.5009	7.79	8.32
	Core	1.5571	1.5024	7.99	8.57
140°C 4 h	Skin	1.5525	1.4997	9.49	7.99
	Mean	1.5533	1.5005	9.49	8.04
	Core	1.5563	1.5025	9.67	7.99
140°C 8 h	Skin	1.5592	1.5019	7.83	8.69
	Mean	1.56	1.5026	7.88	8.76
	Core	1.5632	1.5052	7.67	8.88

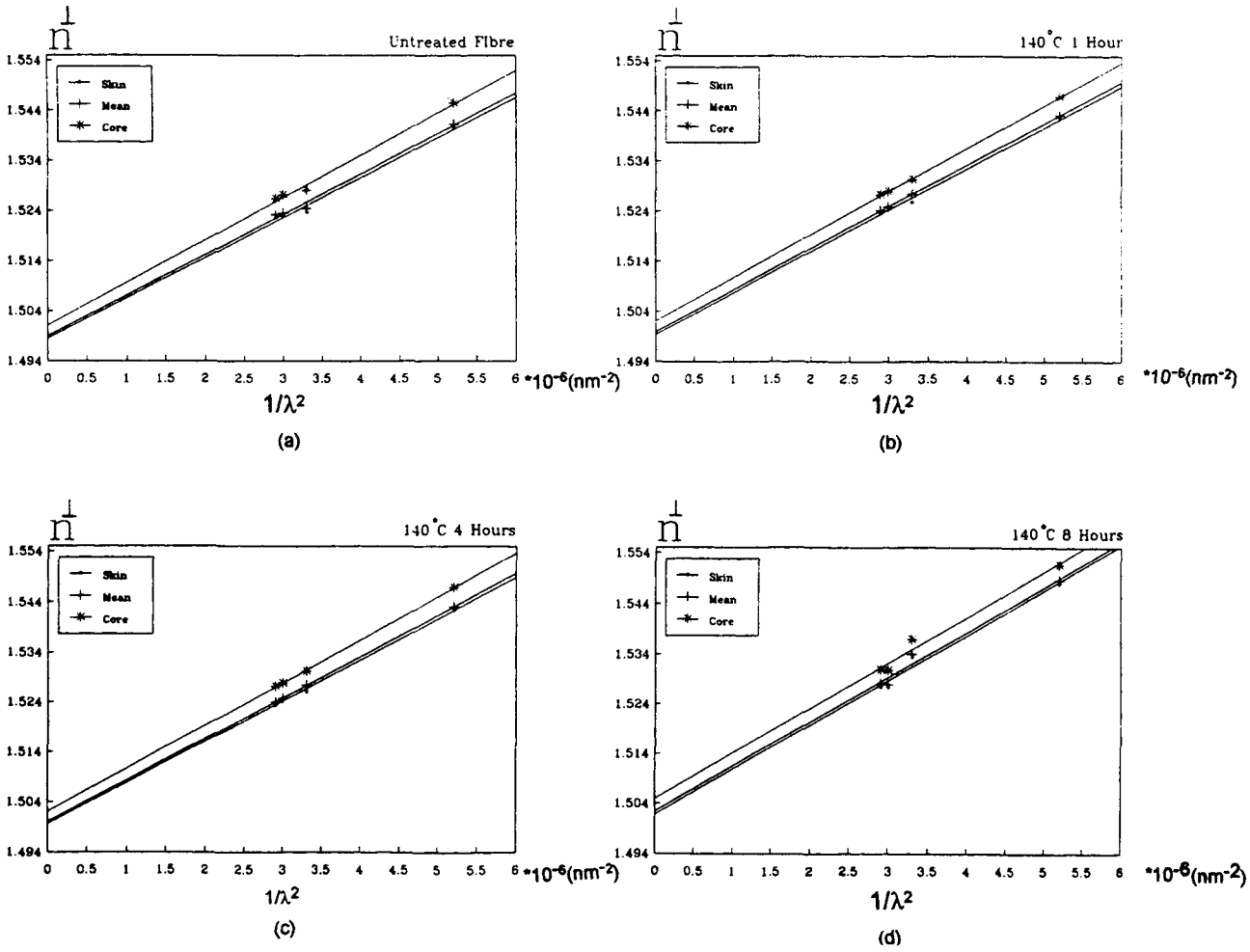

Figure 9 (a–d) Variation of $n_s^{\perp}$, $n_c^{\perp}$, and $n_a^{\perp}$ with $1/\lambda^2$.

Table IV Average Value of Dispersive Power of Unannealed and Annealed Nylon 66 Fibers

State	Layer	$dn^{\parallel}/d\lambda$	$dn^{\perp}/d\lambda$
Unannealed	Skin	-5.27×10^{-5}	-9.81×10^{-5}
	Mean	-4.47×10^{-5}	-9.87×10^{-5}
	Core	-4.78×10^{-5}	-1.03×10^{-4}
140°C 1 h	Skin	-9.62×10^{-5}	-1.01×10^{-4}
	Mean	-9.57×10^{-5}	-1.02×10^{-4}
	Core	-9.81×10^{-5}	-1.05×10^{-4}
140°C 4 h	Skin	-1.17×10^{-4}	-9.81×10^{-5}
	Mean	-1.17×10^{-4}	-9.87×10^{-5}
	Core	-1.19×10^{-4}	-9.81×10^{-5}
140°C 8 h	Skin	-9.62×10^{-5}	-1.07×10^{-4}
	Mean	-9.68×10^{-5}	-1.08×10^{-4}
	Core	-9.42×10^{-5}	-1.09×10^{-4}

also specifications of the unit cell of the crystalline part of the medium.[16] Hannes[16] used the following formula:

$$n_{\text{iso}} = \tfrac{1}{3}(n^{\parallel} + 2n^{\perp}) \tag{8}$$

to estimate a relationship showing the crystallization in homogeneity for some types of polymers. The obtained values of $n_s^{\parallel}$, $n_s^{\perp}$, $n_c^{\parallel}$, $n_c^{\perp}$, $n_a^{\parallel}$, and $n_a^{\perp}$ from the interferometric techniques are used with eq. (8) to determine the isotropic refractive index values for annealed nylon 66 fibers.

Figure 12(a–f) shows the variation of n_{iso} of nylon 66 fibers due to changing annealing times and constant annealing temperatures. The obtained curves reflect that $n_{(\text{iso})s}$, $n_{(\text{iso})c}$, and $n_{(\text{iso})a}$ vary through the first 2 h of annealing temperatures.

Figure 13(a–f) shows that the isotropic refractive

Table V Calculated Values of Polarizabilities per Unit Volume and Isotropic Refractive Indices of Unannealed Nylon 66 Fibers at Room Temperature of 25 ± 1°C

Temperature	$p_s^{\parallel}$	$p_s^{\perp}$	Δp_s	$p_c^{\parallel}$	$p_c^{\perp}$	Δp_c	$p_a^{\parallel}$	$p_a^{\perp}$	Δp_a	$n_{(iso)s}$	$n_{(iso)a}$	$n_{(iso)c}$
25°C	0.0793	0.073	0.0063	0.0799	0.0734	0.0065	0.0795	0.0731	0.0064	1.5422	1.5429	1.47

index of annealed nylon 66 fibers increased by increasing the annealing temperatures at different constant times. The obtained curves reflect that temperatures from 100–140°C for 1 and 2 h means that the isotropic medium is affected by the isothermal changes in these ranges for rearrangement of the segmental breakage chain inhomogeneity.

CONCLUSION

From the measurements carried out in the present work to investigate the change in optical properties due to the annealing process for nylon 66 fibers at different conditions of temperature and time, the following conclusions may be drawn:

1. The effect of the annealing process on nylon 66 fibers depends on the time period and the temperature of annealing.
2. The direction dependence of the refractive indices have unequal behavior in different directions. Clearly, this behavior is proof that the structure of the fiber along its axis is different from that across its axis. The arrangement of the linear molecules of which it is composed are different in the parallel direction from that in the perpendicular one (see Figs. 2–5).
3. The use of multiple-beam Fizeau fringes verifies the Cauchy's dispersive formula and determines the constants A and B of this formula for each layer of the fiber.
4. Change in n_{iso} with different annealing conditions indicates a change in the specific volume of nylon 66 fibers on the annealing process.
5. The variation of the isotropic refractive indices is related to the degree of order orientation and mass redistribution of the sample.
6. The annealing process affects other physical properties (swelling, dyeability, electrical, color, mechanical, etc.); further studies are needed to detect which properties are improved by annealing.
7. The produced microinterferograms clarify the difference in optical path variations due to annealed and unannealed fibers.
8. Reliable results are obtained using multiple-beam Fizeau fringes in transmission for studying thermal birefringence in polymeric fibers, where sharp fringes enable one to determine accurately the refractive indices of any layer of a multilayer fiber.

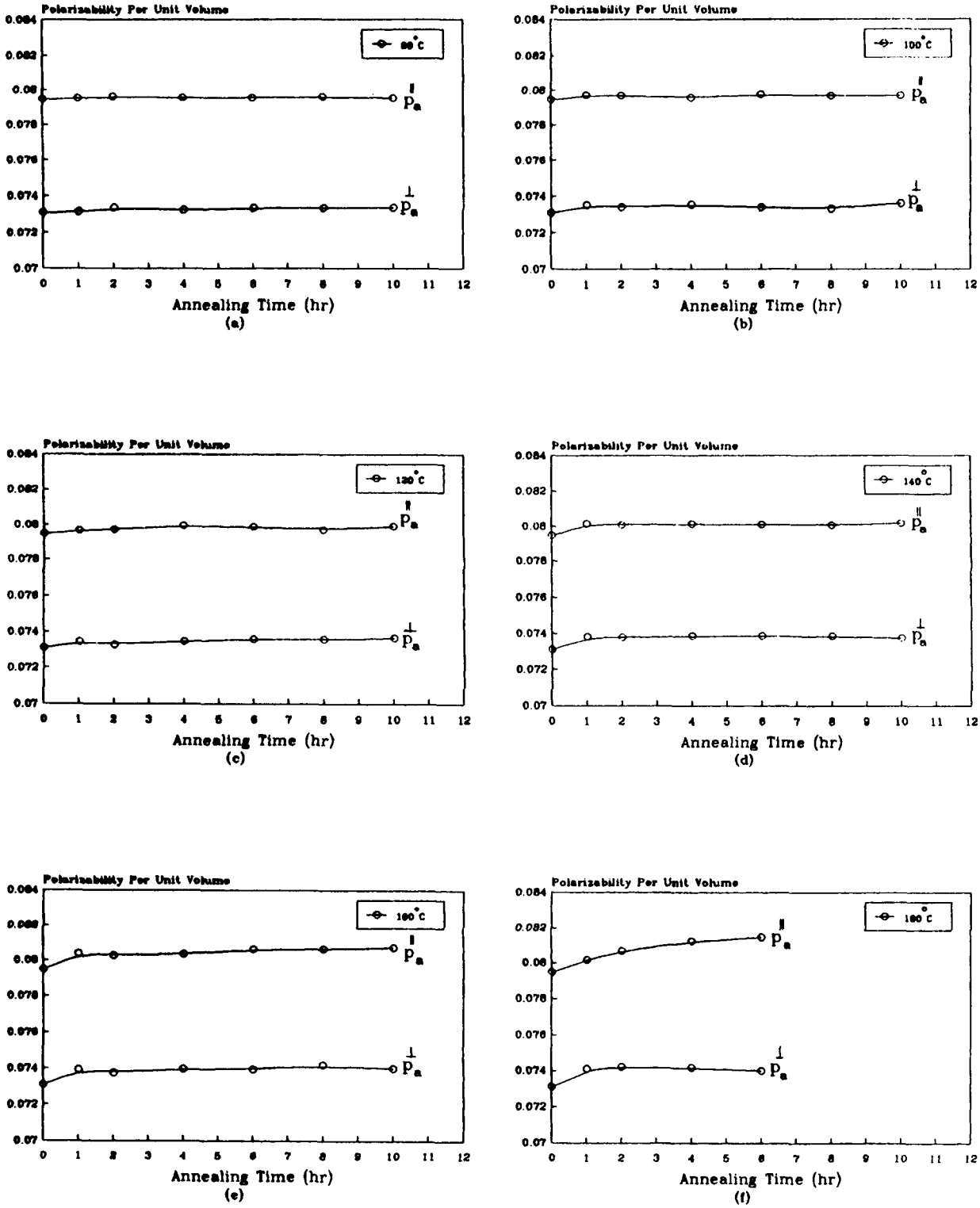

Figure 10 (a–f) Relation between annealing time (1–10 h) and polarizability per unit volume $P_a^{\parallel}$ and $P_a^{\perp}$ at constant annealing temperature (80, 100, 120, 140, 160, and 180°C).

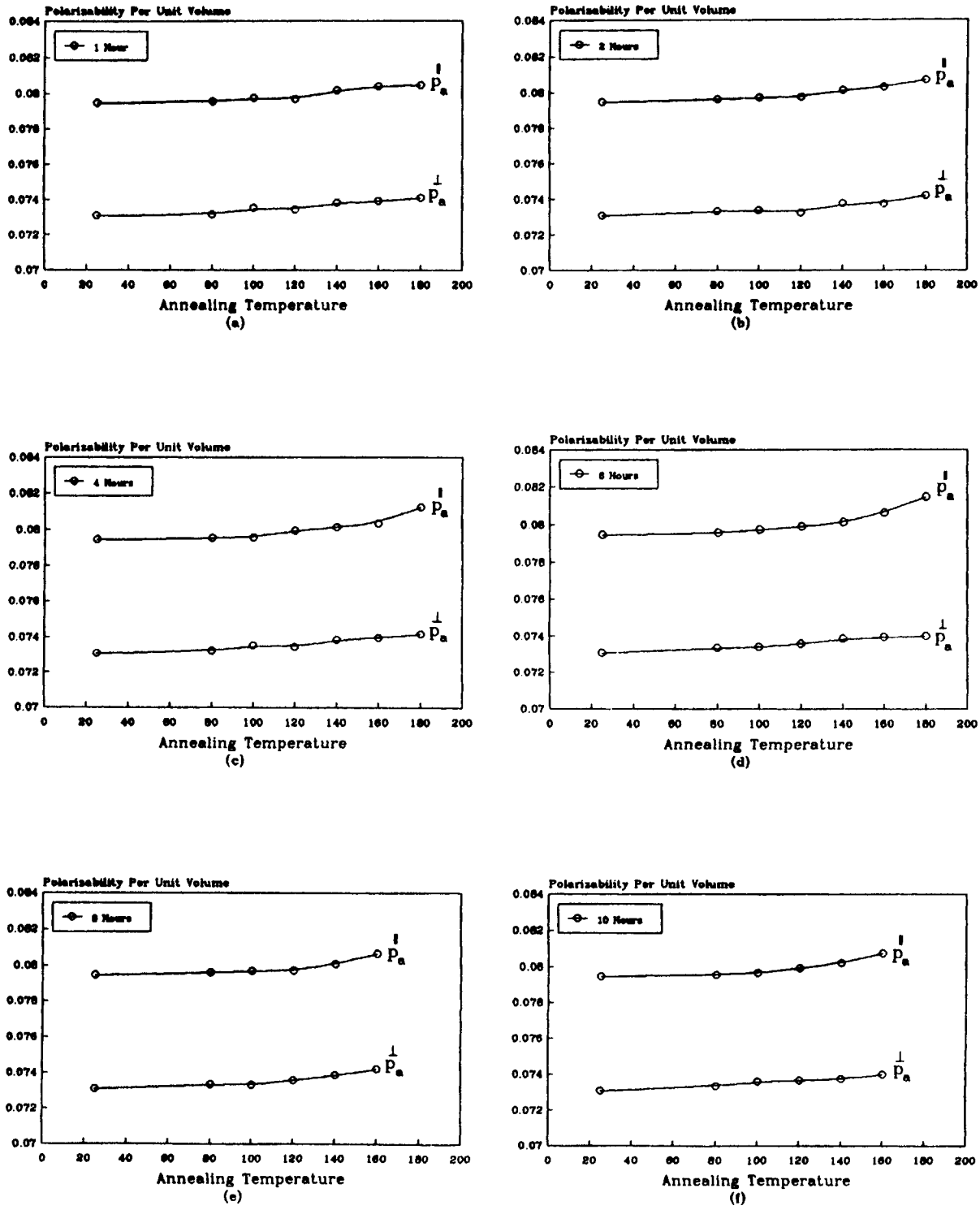

Figure 11 (a–f) Relation between annealing temperature (80–180°C) and polarizability per unit volume $P_a^{\parallel}$ and $P_a^{\perp}$ at constant annealing time (1, 2, 4, 6, 8, and 10 h).

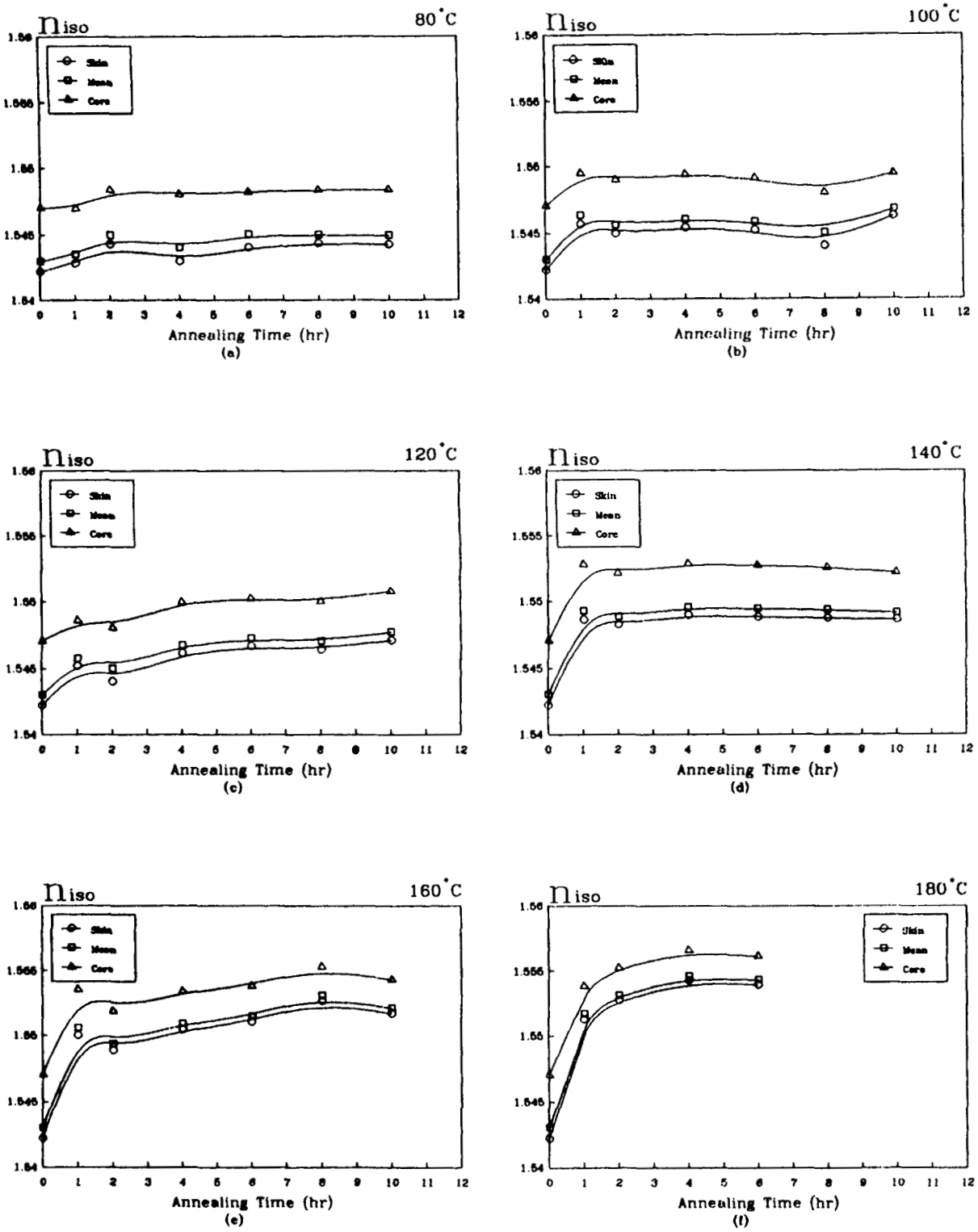

Figure 12 (a–f) Relation between annealing time (1–10 h) and isotropic refractive index $n_{(iso)s}$, $n_{(iso)c}$, and $n_{(iso)a}$ at constant annealing temperature (80, 100, 120, 140, 160, and 180°C).

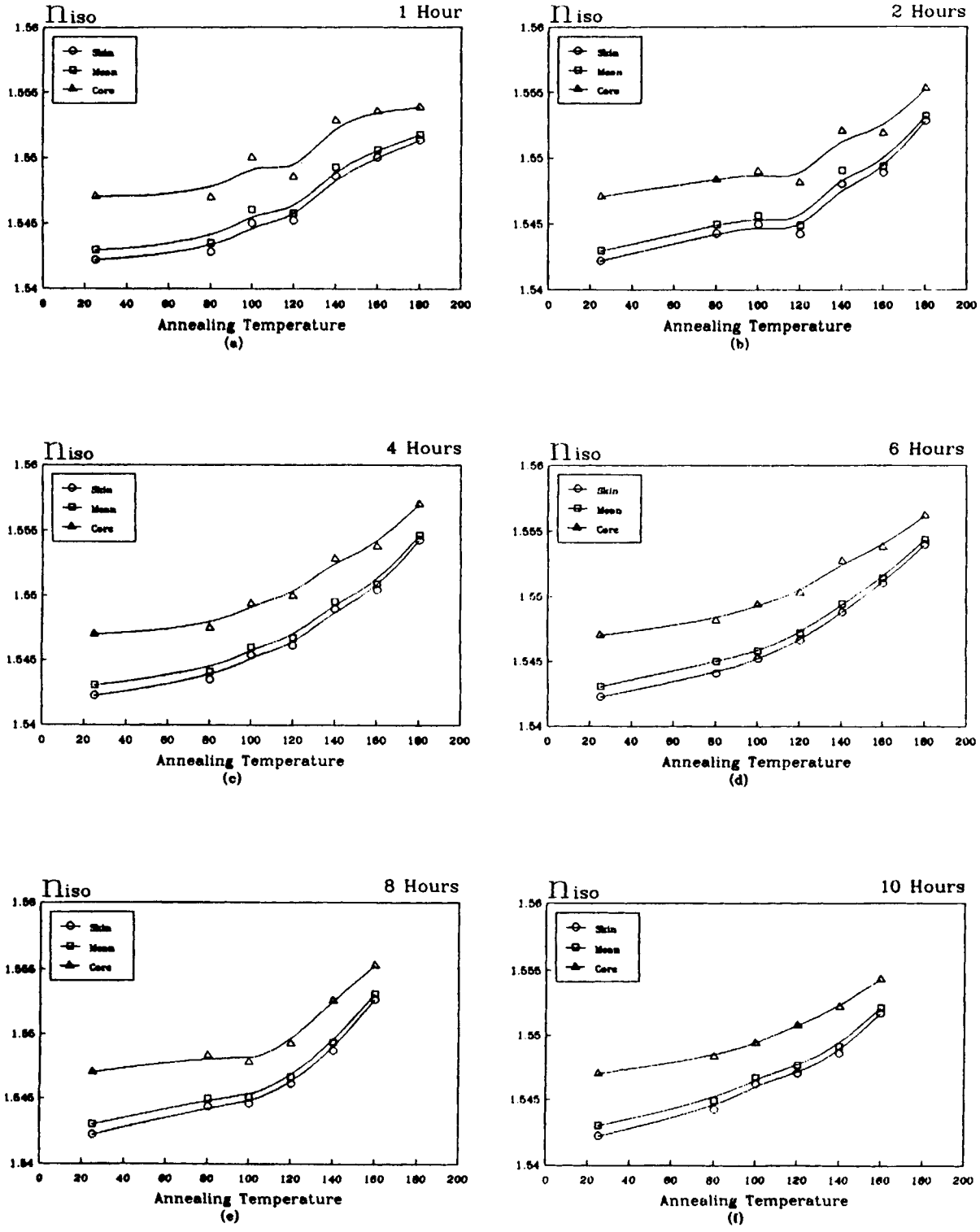

Figure 13 (a–f) Relation between annealing temperature (80–180°C) and isotropic refractive index $n_{(iso)s}$, $n_{(iso)c}$, and $n_{(iso)a}$ at constant annealing time (1, 2, 4, 6, 8, and 10 h).

9. The crystalline parameters of the material varied systematically with annealing temperature.
10. The detailed annealing study revealed continuous changes in the crystalline state; this emphasizes the variations of Δn_s, Δn_c, and Δn_a.
11. The value of the swelling factor for different liquids depends on the time and the temperature of annealing and also on the chemical concentrations of the absorbent and the degree of crystallinity of the fiber.
12. The absorption factor is an indicator of the degree of crystalline and amorphous areas in the structure of the studied fiber.

We conclude from the above results and considerations that the practical importance of these measurements provide acceptable results for the optothermal parameters. Since $n_s^{\parallel}$, $n_c^{\parallel}$, $n_a^{\parallel}$, $n_s^{\perp}$, $n_c^{\perp}$, $n_a^{\perp}$, Δn_s, Δn_c, Δn_a, n_{iso}, $P_a^{\parallel}$, and $P_a^{\perp}$ are a sequence of the material annealed, so the reorientation of the nylon 66 fibers may occur not only during manufacture but also due to the annealing process. Also, it is clear that multiple-beam techniques are useful to clarify the mechanism of the optical behavior of the skin–core structure of nylon 66 fibers with the annealing process. In conclusion, the structure orientation changes due to the annealing process as observed by multiple-beam Fizeau fringes is very promising and further study is required in areas which have not yet been explored.

REFERENCES

1. N. Barakat and A. A. Hamza, *Interferometry of Fibrous Materials,* Adams Hilger, Bristal, 1990.
2. R. M. Moncrieff, *Man-made Fibres,* New Nes-Butterworths, London, 1975, pp. 77–79.
3. S. R. Cockett, *An Introduction to Man-made Fibers,* Sir Isaac Pitman, London, 1966, p. 21.
4. H. W. Wayckoff, *J. Polym. Sci.,* **62,** 83 (1962).
5. S. N. Murthy, H. Minor, and A. Latif, *J. Macromol. Sci. Phys. B,* **26**(4), 427 (1987).
6. I. M. Fouda and M. M. El-Tonsy, *J. Mater. Sci.,* **25,** 4752 (1990).
7. I. M. Fouda, M. M. El-Tonsy, and A. M. Shaban, *J. Mater. Sci.,* **26,** 5052 (1991).
8. O. W. Statton, *J. Polym. Sci. Part A2,* **10,** 1587 (1972).
9. D. Hofmann, R. Leonhardt, and P. Weigel, *J. Appl. Polym. Sci.,* **46,** 1025 (1992).
10. A. E. Zachariodes and S. R. Peter, *The Strength and Stiffness of Polymers,* Marcel Dekker, New York, Basel, 1983, p. 121.
11. S. M. Cury and A. L. Schawalow, *Am. J. Phys.,* **42,** 12 (1974).
12. I. M. Fouda, T. El-Dessouki, and K. A. El-Farahaty, *Ind. J. Text. Res.,* **13,** 11 (1988).
13. N. Barakat and H. A. El-Hennawi, *Text. Res. J.,* **41,** 391 (1971).
14. M. M. El-Nicklawy and I. M. Fouda, *J. Text. Inst.,* **71,** 257 (1980).
15. V. Jindrcii, B. Brancik, and A. Datyner, *Text. Res. J.,* **47,** 662 (1977).
16. H. Hannes, *Z. Z. Kolloid. Polym.,* **25,** 765 (1972).

Received April 26, 1995
Accepted October 6, 1995